Coherence Optimization of Vertical Cavity Semiconductor Optical Amplifiers

Michael Sánchez[*a], Pengyue Wen[a], Matthias Gross[a], Osman Kibar[a], Sadik C. Esener[a]

[a]Electrical and Computer Engineering Dept., University of California - San Diego

ABSTRACT

Vertical cavity semiconductor optical amplifiers (VCSOAs) are attractive devices for use in coherent optical amplification, especially where 2-D amplifier arrays are required. However, the coherence preservation quality of a VCSOA depends strongly on the bias condition, resonant wavelength mismatch, and the optical input power level. We characterize the coherence degree of a VCSOA as a function of these parameters by measuring interference fringe visibility with an interferometer. The dominant factors influencing the contrast of the fringes are the ratio of coherent, stimulated emission photons to amplified spontaneous emission (ASE) photons, and the spectral distortion of the amplified signal. Mostly, the overall gain and the saturation characteristic of the amplifier determine the ratio of stimulated emission to ASE. The spectral distortion of the signal is due to the narrow gain window of the VCSOA, but the effect significantly degrades the visibility only for relatively large wavelength mismatch from the gain peak. Analytic expressions may be used to identify the optimal bias current and optical input power to maximize the amplifier gain and visibility of the interference.

Keywords: VCSOA, coherent array, ASE, optical amplifier

1. INTRODUCTION

The vertical cavity semiconductor optical amplifier (VCSOA) is emerging as a potentially attractive device for applications such as pre-amplification and optical modulation[1]. The VCSOA is essentially a vertical cavity surface emitting laser (VCSEL) biased below the lasing threshold. Under these conditions, the VCSEL becomes a Fabry-Perot laser amplifier with very high mirror reflectivities. One of the principal advantages of the VCSOA compared to other SOAs is the potential fabrication of two-dimensional arrays of devices. The ability to create planar 2-D arrays of amplifiers allows a variety of new ideas to be considered. One such possibility is the creation of coherent, optical phase-locked arrays using VCSOAs[2]. Such arrays could be used for coherent information processing, beamsteering[3], and coherent detection, among others. VCSOA arrays have several other attractive qualities as well. The array can be large in size, limited only by thermal management issues[4,5] and the fan-out (i.e. power) of the input signal. The circular geometry of the devices allows efficient coupling to and from fiber or free space optics. The relatively large pitch, typically 250μm, of the devices in an array should ease the design of an optical system for input/output. That is, the larger the pitch, the further away the first set of optics can be placed without significant overlap between the signals from adjacent elements. VCSOAs exhibit a very narrow gain window, because of the high Q of the Fabry-Perot cavity. This characteristic may be exploited as an effective filter for noise or in WDM environments. Additionally, the small active area of the device allows operation with low power consumption, typically on the order of 10mW. Finally, the small size of the device should allow for high-speed modulation, as demonstrated by commercial VCSEL products with direct modulation speeds of 10Gb/s.

Several of the device characteristics listed above result in trade-offs that must be considered in the design of any system using VCSOAs. First, the narrow gain window makes the device very sensitive to any physical phenomenon that alters the effective optical length of the laser cavity. Such a perturbation will shift the resonant frequency and cause a change in the gain of the amplifier because it changes the alignment of the device resonance with the source signal. Possible sources of such a misalignment include fluctuations in temperature, bias current, or wavelength drift of the source laser itself. A second consequence of such a narrow gain bandwidth is the possibility of signal distortion. If the input signal has a bandwidth comparable to the amplifier gain window, the spectrum will be unequally amplified. Generally, this

---

[*] Correspondence: mdsanchez@ucsd.edu, UCSD ECE Dept. 0407, 9500 Gilman Dr., La Jolla, CA 92093-0407

Report Documentation Page		Form Approved *OMB No. 0704-0188*

Public reporting burden for the collection of information is estimated to average 1 hour per response, including the time for reviewing instructions, searching existing data sources, gathering and maintaining the data needed, and completing and reviewing the collection of information. Send comments regarding this burden estimate or any other aspect of this collection of information, including suggestions for reducing this burden, to Washington Headquarters Services, Directorate for Information Operations and Reports, 1215 Jefferson Davis Highway, Suite 1204, Arlington VA 22202-4302. Respondents should be aware that notwithstanding any other provision of law, no person shall be subject to a penalty for failing to comply with a collection of information if it does not display a currently valid OMB control number.

1. REPORT DATE **01 JUN 2005**	2. REPORT TYPE **N/A**	3. DATES COVERED **-**	
4. TITLE AND SUBTITLE **Coherence Optimization of Vertical Cavity Semiconductor Optical Amplifiers**		5a. CONTRACT NUMBER	
		5b. GRANT NUMBER	
		5c. PROGRAM ELEMENT NUMBER	
6. AUTHOR(S)		5d. PROJECT NUMBER	
		5e. TASK NUMBER	
		5f. WORK UNIT NUMBER	
7. PERFORMING ORGANIZATION NAME(S) AND ADDRESS(ES) **Electrical and Computer Engineering Dept. University California San Diego 9500 Gilman Drive, La Jolla, CA92093-0407**		8. PERFORMING ORGANIZATION REPORT NUMBER	
9. SPONSORING/MONITORING AGENCY NAME(S) AND ADDRESS(ES)		10. SPONSOR/MONITOR'S ACRONYM(S)	
		11. SPONSOR/MONITOR'S REPORT NUMBER(S)	
12. DISTRIBUTION/AVAILABILITY STATEMENT **Approved for public release, distribution unlimited**			
13. SUPPLEMENTARY NOTES **See also ADM001923.**			
14. ABSTRACT			
15. SUBJECT TERMS			

16. SECURITY CLASSIFICATION OF:			17. LIMITATION OF ABSTRACT **UU**	18. NUMBER OF PAGES **10**	19a. NAME OF RESPONSIBLE PERSON
a. REPORT **unclassified**	b. ABSTRACT **unclassified**	c. THIS PAGE **unclassified**			

Standard Form 298 (Rev. 8-98)
Prescribed by ANSI Std Z39-18

filter effect is beneficial, but it could have detrimental effects under certain conditions. Another problem is the small size of the device. While this feature allows for low current, high-speed operation, it also leads to a low saturation power and thus a significant dependence of the gain on the input power level. Finally, the current bias condition is important, since that controls the carrier density in the active region, which in turn influences the optical gain and amount of spontaneous emission (SE) generated.

In coherent arrays based on VCSOAs, two parameters are of most interest. First, the degree of correlation between two or more amplified signals, i.e. the degree of coherence, is of paramount importance. Secondly, the optical gain of the amplifier should be as large as possible, so that a single source can be distributed to many array elements. In this paper, the degree of coherence of a VCSOA signal is characterized and modeled as a function of bias current, optical input power and resonant wavelength mismatch. These results are combined with observations of device gain to determine the optimal operation conditions for VCSOAs in coherent arrays. Suitable limits and ranges are determined for bias current, optical input power level, and wavelength.

2. THEORY

2.1. Partially Coherent Amplified Signal

Like any semiconductor optical amplifier (SOA), the VCSOA generates amplified spontaneous emission (ASE) which will be mixed with the amplified signal. The amplifier output photons will be partitioned between a coherent fraction generated by stimulated emission induced by the signal, and some incoherent fraction of ASE and SE photons. The coherence degree is treated as a statistical term, where photons are either correlated or not. Then the total optical power can be divided between those photons that are correlated to each other and those that are essentially random. All the optical power emitted as spontaneous emission is assumed to have no relationship to the input signal, or with itself. This assumption is reasonable as long as the integration period of our observation is long compared to the coherence time of the spontaneous emission. Experimental measurement of the fringe pattern from the spontaneous emission shows a degree of coherence less than 0.1. Expressed mathematically, the optical power will be a sum of coherent and incoherent parts:

$$P = AP_c + BP_{ic} \tag{1}$$

In this experiment, the light consists of the amplified light and spontaneous emission:

$$I_1 = |g|_p I_{out} + (1 - |g|_p) I_{out} + I_{sp} \quad , \quad I_2 = CI_1 \quad , \quad C \leq 1 \tag{2}$$

The first term is the coherent portion, and the second two terms are the random phase fraction that will not contribute to any interference pattern. I_1 and I_2 represent the intensity of two fields of identical composition. I_{out} represents the amplified signal intensity, I_{sp} is the spontaneous emission intensity, and $|g|_p$ is the coherence degree of the passive system. The visibility of an interference pattern from these two beams can be derived using the interference law for partially coherent light[6]:

$$I = I_1 + I_2 + 2\sqrt{I_1 I_2} \, \text{Re}[g_{12}(\tau)] \tag{3}$$

Combining Eqn.2 with Egn.3 and the definition of visibility, eqn.4 is obtained:

$$V = \frac{I_{max} - I_{min}}{I_{max} + I_{min}} = \frac{2\sqrt{C} \, |g|_p \, I_{out}}{I_1 + I_2} \quad \propto \quad \frac{|g|_p}{1 + {I_{sp}}\big/{GI_{in}}} \tag{4}$$

If we characterize the gain (G), spontaneous emission, and the passive coherence degree, then we can make a prediction about the expected visibility.

2.2. Spontaneous Emission

This theory is complicated by the fact that the ASE output may not be a constant for all conditions. Obviously, the spontaneous emission rate will be a function of the bias condition, but it also may be altered by the injection of photons

from an external source. This effect has been observed in other types of SOAs, and several theoretical explanations exist in the literature[7,8,9,10]. The basic premise behind this phenomenon is that the injected photons increase the photon density inside the cavity. The carrier consumption rate is then increased because of stimulated emission and the equilibrium carrier density decreases. The spontaneous emission rate follows the carrier density proportionally. The approach of Obermann, et. al.[10], may be adapted to describe a VCSOA. The starting point is the steady state rate equations for a travelling wave SOA:

$$\frac{dP}{dz} = [\Gamma g(n,\lambda) - \alpha]P(z) = 0 \quad , \quad \frac{dn}{dt} = \frac{I_{eff}}{eV} - \frac{n}{\tau_s} - S(ASE) - \frac{\Gamma g(n,\lambda)}{Ahc/\lambda}P(z) = 0 \tag{5}$$

Where Γ is the confinement factor, $g(n,\lambda)$ is the material gain coefficient, α is the internal loss coefficient, $P(z)$ is the optical field in the amplifier, V is the volume of the device, A is the area of the active region, τ_s is the non-radiative recombination lifetime, h is Plank's constant, and c the speed of light. The term S(ASE) accounts for carrier consumption by ASE. To simplify these equations, several assumptions are made[1]. First, the gain coefficient is assumed to be much larger than the internal loss coefficient, so $\alpha=0$. Also, the consumption of carriers by ASE is assumed to be a minor process compared to the other three terms in the carrier density rate equation, so S(ASE)=0. The gain coefficient is approximated as a linear function:

$$g(n,\lambda) = g_0(\lambda)[n - n_{tr}(\lambda)] \tag{6}$$

Where n_{tr} represents the carrier density at transparency. Using these assumptions, the set of equations can be solved for the steady state condition and an expression for the carrier density can be obtained:

$$n(z) = n_{tr}(\lambda) + \frac{I_{eff}\tau_s/eV}{1 + x(z)} \quad , \quad x(z) = \frac{P(z)}{P_{sat}} \quad , \quad P_{sat} = \frac{Ahc}{\Gamma\lambda\tau_s g_0(\lambda)} \tag{7}$$

The active region of a VCSOA is very thin, so eqn. 6 is to be evaluated at a single z-axis location. The carrier density is dependent on the optical power inside the amplifier, and thus on the optical input power and coupling efficiency. At this point, another equation is introduced. The ASE power emitted from an SOA is modeled by the following equation[10]:

$$W_{ASE} = \frac{hc}{\lambda}\eta_{sp}(n)[G(n,\lambda) - 1] \quad , \quad \eta_{sp}(n) = n/(n + n_{tr}) \tag{8}$$

Where $G(n,\lambda)$ is the usually the single-pass gain, and η_{sp} is the population inversion parameter. In the case of a VCSOA, the photons make multiple round trips through the amplifier, so the single-pass gain cannot be used here. Instead, the overall gain of the amplifier should be applied.[11] Figure 1 plots the measured gain of a VCSOA device vs. optical input power, with a curve fit though the data points. The fitting curve is generated using the common expressions for the gain of a Fabry-Perot amplifier[12]. The second solid curve is an arbitrarily scaled plot of the ASE power (Eqn. 8), using the same parameters as the fitting curve. The dashed line is a scaled copy of the gain curve.

The close agreement of the ASE curve and the scaled copy of the gain curve demonstrates the population inversion parameter exerts only minor influence at a given bias current. Therefore, the ASE emission may be assumed to be proportional to the gain, and the population inversion parameter will be approximated as a constant value. The major conclusion here is that if a curve can be fitted to the gain saturation data, a scaled replica of that curve may be used to model the ASE power Vs. P_{in}. For a VCSOA, the gain saturation at a given bias current can be fit with an equation of the form of Eqn.7. Therefore, the visibility can be predicted without knowing all the device structure details, but simply the form of the gain vs. input power.

A functional form for the ASE and SE emission vs. bias current is also needed. Typically, this output can be calculated from the rate equations[13], but a simpler, analytic approximation is desirable. There should be two contributions to the optical field emitted from a VCSOA. First, spontaneously generated photons that exit the cavity directly without reflection. The second contribution is the SE photons that are reflected back into the cavity and amplified, i.e. the ASE. The output without optical injection should then be a sum of these two terms. The SE may be considered as directly proportional to the carrier density in the device, and the ASE can be obtained using Eqn. 8. To apply these equations, it
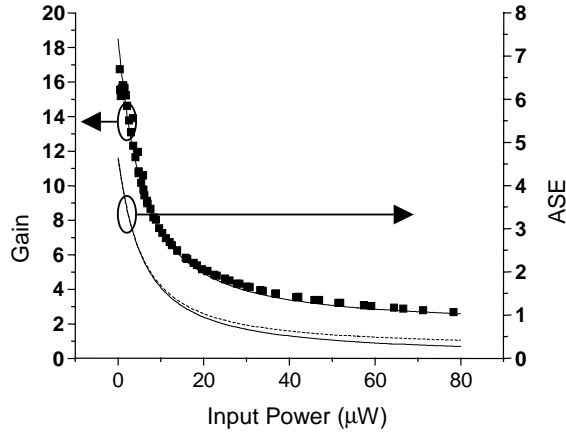
Figure 1: Gain saturation and ASE output vs. input power. Dots are experimental measurements of gain w/ fitting curve. Second solid line is result of Eqn.8. Dashed line is scaled replica of gain curve.
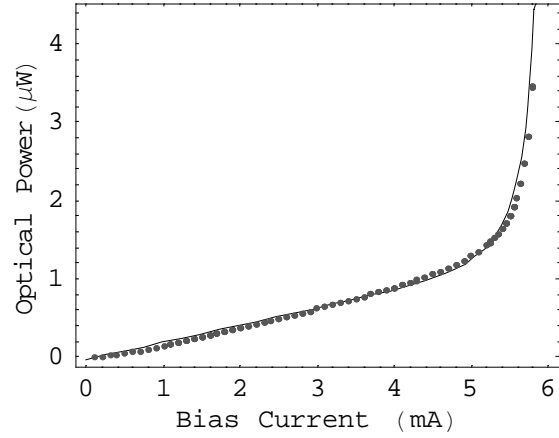
Figure 2: Output power from VCSOA and fitting curve from Eqn. 9.

is necessary to introduce the approximation that the carrier density is linearly related to the bias current. Then the total emitted power can be given by:

$$P_{sp} = A*I + B[G(I,\lambda)-1] \tag{9}$$

Where A and B are fitting parameters. Fig. 2 shows eqn. 9 fit to measured data from one of the VCSOAs used in our experiments. The optical power can be translated to intensity through measurement of the beam profile, since total power is just the integration of intensity over an area.

To summarize, the spontaneous emission intensity used in eqn. 4 may be calculated using the above equations as a function of bias current, optical input power, and wavelength mismatch (via coupling efficiency).

2.3. Spectral Distortion

A final consideration is the spectral distortion introduced by the VCSOA. The linewidth of the amplified signal may not be the same as the original signal, and this can alter the interference of two fields when the path lengths are not equal. To explore this idea and its contribution to the observed behavior, the spectral distortion model is developed. The premise is straightforward. The input power spectrum will be modified because of the narrow bandwidth of the VCSOA. That is, each frequency component will be amplified according to the gain of the amplifier at that frequency. The spectrum of the amplified light will then be the product of the spectral gain window of the VCSOA and the input spectrum. The resultant linewidth and position of the peak frequency are the two parameters of interest. The gain spectrum of the VCSOA should be dominated by the frequency response of the Fabry-Perot cavity, and have a form:

$$g_a(v) = \frac{(1-R_1)(1-R_2)G_s}{(1-\sqrt{R_1 R_2}G_s)^2 + 4\sqrt{R_1 R_2}G_s \sin^2\left(\frac{2\pi x}{v_0}\right)} \tag{10}$$

Here $x = v-v_0$, v_0 is the peak frequency of the gain spectrum. R_1 and R_2 are the top and bottom mirror reflectivities, and G_s represents the single pass gain coefficient. For our input, we assume the Lorentzian lineshape typical of semiconductor lasers:

$$f(v) = \frac{\Delta v}{2\pi\left((x - dv)^2 + \left(\dfrac{\Delta v}{2}\right)^2\right)}$$

(11)

The linewidth of the laser is Δv, and x is the same as in Eqn. 10. The displacement of the input spectrum from the VCSOA resonance is included via the "dv" term. The product of these two lineshapes is generally difficult to treat analytically, since it involves high order polynomials in the denominator. We have written a Mathematica script to numerically find the peak wavelength and linewidth for relatively small detunings and otherwise arbitrary conditions. However, in certain cases, we can apply further approximations to simplify the problem and obtain analytic solutions as well. In particular, for small ($2\pi x \ll v_0$) excursions from central peak, the $\sin^2$ term in Eqn. 10 can be approximated as the argument squared (small-angle approximation). After some algebraic manipulation, eqn. 10 can then be rewritten as a function of the full width at half-maximum (FWHM) of the gain spectrum, Δv_a:
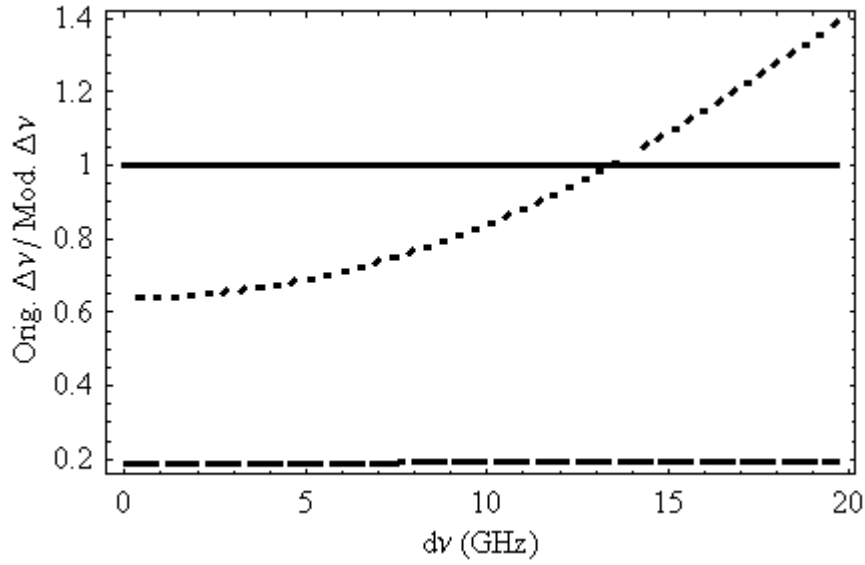
$$g_a(v) = \frac{(1 - R_1)(1 - R_2)}{4\pi^2 R_1 R_2} \frac{v_0^2}{4(v - v_0)^2 + \Delta v_a^2} \quad , \quad \Delta v_a = \frac{v_0\left(1 - G_s\sqrt{R_1 R_2}\right)}{2\pi\sqrt{R_1 R_2}}$$

(12)

The first limiting case is for the input linewidth to be much less than the amplifier linewidth. In this case the VCSOA will behave much like any other SOA, and there should be little distortion. The gain will not vary significantly over the frequency range of the input signal and the output should be nearly identical in spectral content. Mathematically, eqn 12 reduces to a constant value (to first order) within the interval $v < \Delta v$ if $\Delta v_a \gg \Delta v$. Fig. 3 plots the peak shift vs. detuning and Fig. 4 plots the FWHM vs. the detuning, as obtained by the Mathematica program. The FWHM is normalized to the original linewidth so that the result from all three cases can be shown on the same plot, where this case is represented by the solid lines. As expected, the peak shift and change in the FWHM is extremely small.

The second case deals with the more realistic circumstance where the linewidths are approximately equal. That is, $\Delta v_a \sim \Delta v$. To deal with this case analytically, we approximate eqn. 10 using eqn. 11. To find the peak wavelength, the denominator should be minimized, and one can derive a cubic equation for the peak frequency. The polynomial is not factorable, but if we make the substitution $x = dv/2*(1 + dx)$, and use binomial expansions on the higher order terms, a linear equation is found. The only solution for is $dx = 0$. So, in this limit, the peak wavelength should halfway between
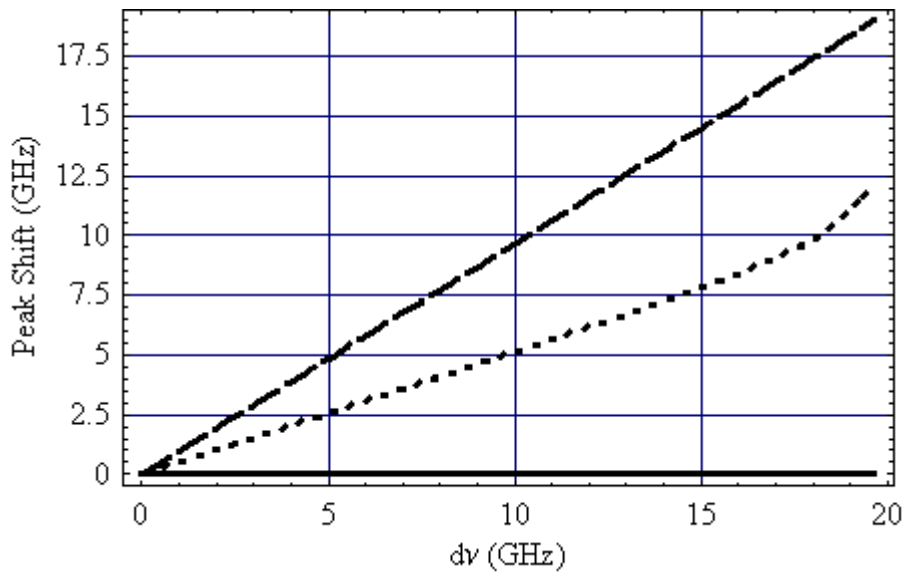
Figure 3: Peak Shift vs. Detuning. Solid: Δv=1 GHz, Dotted: Δv=20 GHz, Dashed: Δv=100 GHz. Δv_a=20 GHz for all three

Figure 4: Linewidth of amplified signal vs. detuning. Linewidth is given as fraction of original. Solid: $\Delta\upsilon=1$ GHz, Dotted: $\Delta\upsilon=20$ GHz, Dashed: $\Delta\upsilon=100$ GHz. $\Delta\upsilon_a=20$ GHz for all three.

the input peak and the VCSOA gain peak. Unfortunately, solving for the FWHM has proven more difficult, and no analytic solution is easily obtained. However, the numerical solution is still quite capable, as shown in Figs. 3 and 4 by the dotted lines. The peak shift is found to have a nearly linear slope of about ½, confirming our assumptions. The FWHM can vary significantly as the detuning parameter in increased, and the deviation accelerates as the detuning increases. Also shown in the figure is the original linewidth (horizontal dashed line). The linewidth of the amplified light is noticeably smaller than the original signal near the resonant wavelength.

The third case occurs in the limit that $\Delta\upsilon_a \ll \Delta\upsilon$, when the input signal linewidth is much broader than the VCSOA spectral window. In this case, the VCSOA will act like a filter, and amplify only a portion of the input signal. Furthermore, the input signal is approximately constant over the bandwidth of the VCSOA. Consequently, the linewidth should closely follow the FWHM of the VCSOA and the peak frequency of the output should be close to the gain peak of the VCSOA. This is shown in Figs. 3 and 4 by the dashed lines. It is unlikely this case would be encountered with coherent arrays, since a narrow linewidth signal is essential to the efficient use of coherent combination of fields.

The degree of coherence is related to the spectral distribution of a signal and path delay through a Fourier transform[6]. In the case of a Lorentzian spectral distribution, the coherence degree is an exponential function of the delay time over the coherence time and the coherence time is the inverse of the FWHM. Thus, the correction due to the spectral distortion can be included as a modification of the passive coherence degree in Eqn. 3. A cautionary note should be included however, that such a simple correction is only valid while the amplified signal maintains an approximately Lorentizan shape. It is expected that this condition could easily be violated, especially for detunings larger than the FWHM.

2.4. Optimization

The calculations outlined above predict the visibility of interference between light beams amplified by a VCSOA as a function of bias current, input power and wavelength. They may be used to identify optimal operation conditions and tolerances for VCSOAs in coherent arrays. Namely, it is desirable to maximize the gain and visibility. The former decreases as input power is increased (Fig. 1), and the latter exhibits the opposite trend (Eqn. 4). Therefore, a maximum should exist in the visibility-gain (VG) product and will be used as the optimization variable. The VG product maximum will identify the optimal input power level to balance gain and visibility. The same product can be used to optimize the

bias condition by maximizing the peak value of the VG product and minimizing the optical power level at which the peak is located. Finally, the variation of the visibility with wavelength mismatch may be used to set limits on wavelength drift and non-uniformity in an array.

3. EXPERIMENTAL SETUP AND RESULTS

3.1. Experimental Setup

Our goal is to characterize the self-coherence of a VCSOA as a function of input power and detuning from the resonance frequency. This can be obtained from an interference fringe pattern created by the setup shown in Fig. 5. A 50/50 BS (#3) divides the VCSOA output, and an adjacent mirror reflects the rest of the light to the same area on a CCD. Because the two beams are slightly tilted with respect to one another, a horizontal fringe pattern is produced. By measuring the visibility of the pattern, the degree of self-coherence can be estimated. The spacing between the mirror and BS #3 is about 1 cm, and the distance to the CCD from BS #3 is 2 m. At these distances, with 850 nm light, the spacing of the fringes is about 80 μm, and is easily resolved by the CCD beam profiler.

The resonant wavelength of the VCSOA was changed by using a thermo-electric heat sink as the mount for the laser diode package. The measured coherence degree is always compared to the reference coherence degree of the passive system. That is, the visibility achieved when the VCSOA is unbiased, or a passive mirror is placed in the system instead of the VCSOA. It is necessary to take this reference measurement to account for wavefront distortions from the optics in the beam path and also the finite bandwidth of our source laser. The system includes a fixed path length difference between the two beams, and so the maximum achievable visibility will be limited according to the linewidth of our light source. The time delay of the setup helps minimize the impact of interference of spontaneous emission with itself. Since the bandwidth of the spontaneous emission is large, the visibility of any such interference should be quite low relative to the stimulated emission field. Hence, the dominant effect should be that the overall background level is raised by the spontaneous emission.

The devices used are proton-implanted VCSELs manufactured by EMCORE and designed as transmitters at 850nm. These devices are used are reflection-mode VCSOAs when biased below the lasing threshold. Measurements were conducted using two different aperture sizes, 15um and 8um. The gain window and saturation curves for each device were measured independently of the visibility data, but under identical conditions.
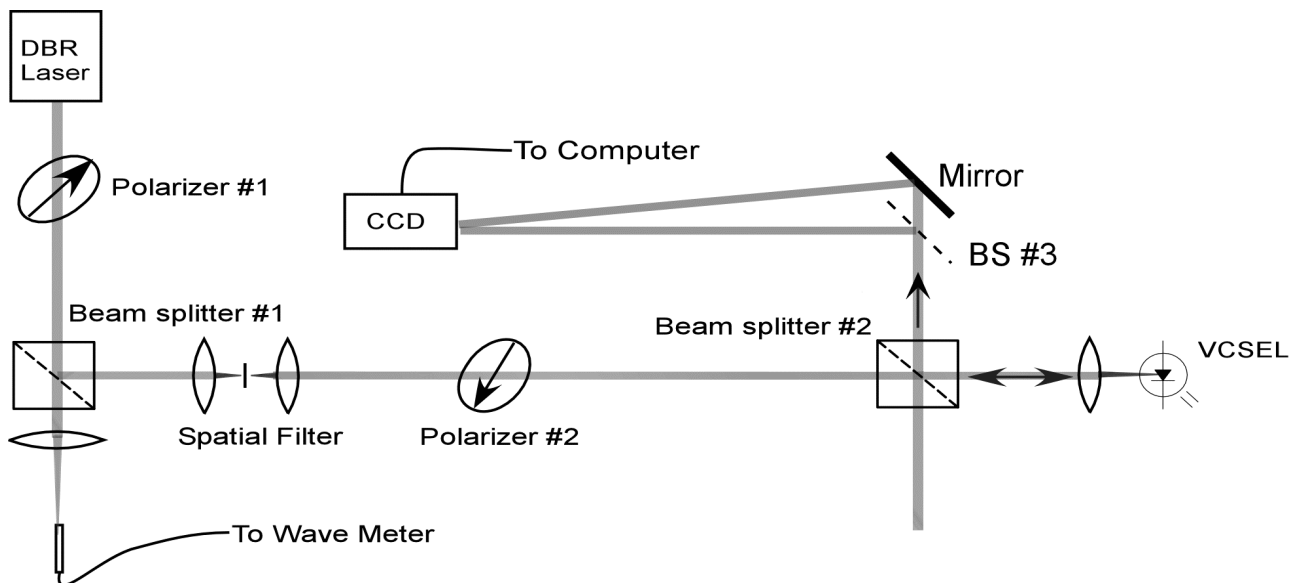
Figure 5: Schematic of Experimental Setup

## 3.2. Visibility Vs. Input Optical Power

The visibility of the fringe pattern is measured while varying the optical input power at the peak gain wavelength. The two beam profiles are also observed, in order to compare the measured result with calculated predictions using Eqn.4. The result is shown in Fig. 6. The dashed line applies no corrections to Eqn.4, treating the SE power as a constant regardless of optical input. The dotted line accounts for the saturation of the SE, using the measured gain saturation data shown in Fig. 1 and the measured SE output from the VCSOA without any optical input. The solid line adds the correction to the visibility due to the spectral distortion of the amplifier. The linewidth of the source laser is estimated using the maximum visibility achieved in the passive system. The linewidth of the VCSOA is taken from measurement of the gain vs. wavelength. The two bandwidths are found to be similar in width, about 10GHz. A new linewidth and maximum visibility is then calculated using the program mentioned in section 2.3. It is notable that the corrections applied do not significantly change the shape of the curve, but rather simply raise the maximum predicted visibility. Good agreement with the measured visibility is found once all the corrections have been included.

3.3. Visibility Vs. Bias Current

The visibility Vs. P_{in} curves are observed at two different bias currents, with the result shown in Fig. 7 on logarithmic scales. The bias current differs by about 3% of the threshold value for the two data sets. The bias current was 8.0 mA for the black dots, and 7.8mA for the gray ones. The solid lines are predicted curves. Here we have used the Fabry-Perot gain equations. The parameters are calibrated by matching the visibility saturation curve at 8.0 mA. The second curve is generated by reducing the bias current in the simulation to 7.8mA, while all other parameters remain unchanged. Apparently, the increase in gain outweighs the increase in the spontaneous emission power. This is sensible, since higher gain will mean the field inside the amplifier will increase toward saturation more quickly with input power than before, while the SE power output is simply increased by some constant amount. The maximum visibility is unchanged by the bias current, since for very large inputs, the coherence degree is limited by the quality of the source laser.

3.4. Visibility Vs. Wavelength Mismatch

The visibility of the fringe pattern is measured while varying the input wavelength, as shown in Fig. 8. The gain window is also recorded, and a normalized plot is shown as the square-data points. The triangles are expected values,
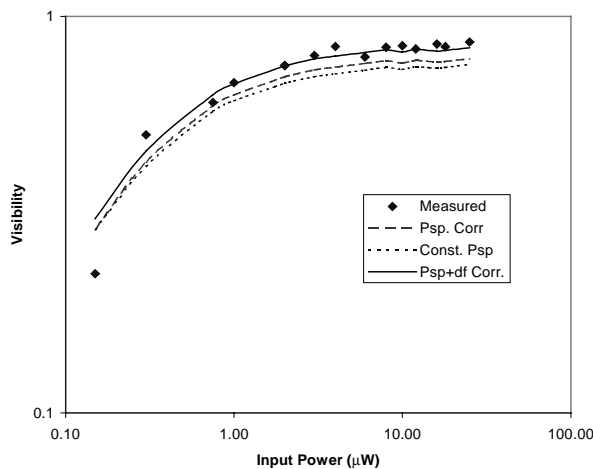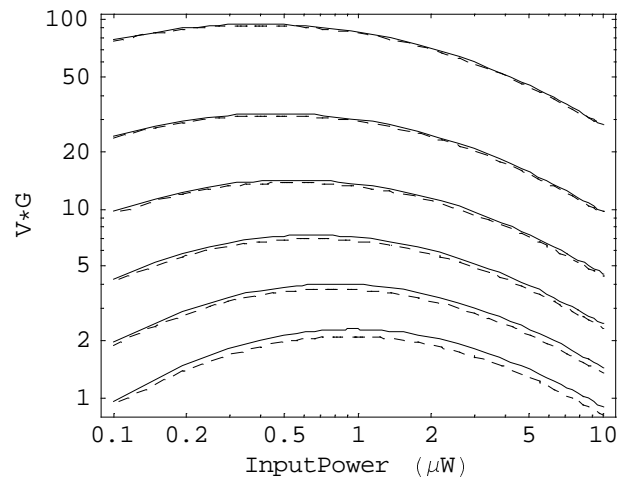

Figure 6: Visibility vs. P_{in}. Dotted line = prediction w/ constant P_{sp}. Dashed = Prediction w/ saturating P_{sp}. Solid = Dashed + spectral distortion
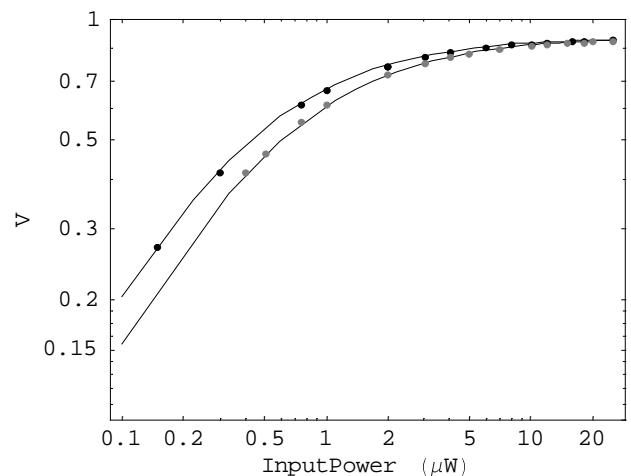
Figure 7: V Vs. P_{in} for I_{bias}=8.0,7.8 mA. Gray dots are 7.8mA data. Solid curves are theoretical fits.
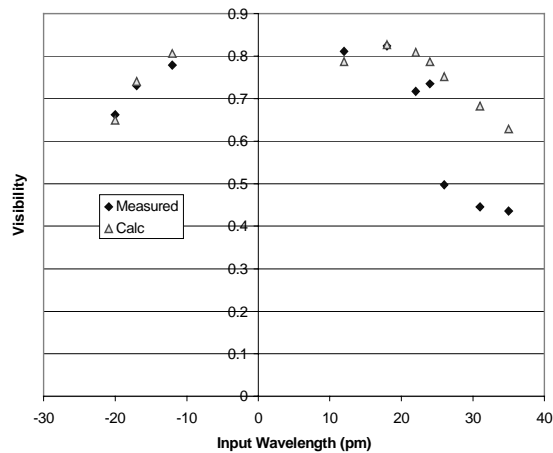
Figure 8: Visibility Vs. Δλ. Diamonds = measured values. Triangles = Calculated values. Squares = normalized gain

Figure 9: Visibility-Gain product Vs. P_{in}. Bottom to top curves are I_{bias}=0.8,0.83,0.86,0.89,0.92,0.95 relative to threshold. Dashed lines count ASE as constant.

based on the individual beam profiles, measured gain values, and estimated spectral distortion at the peak. Correction for the variation in linewidth with detuning is not included, since the difference is not visible in the plot. The reduction in gain with detuning is attributed to a change in coupling efficiency, so I_{in} in Eqn. 4 is reduced proportionally with the measured gain. The agreement between predicted and measured values is good except for detunings larger than 20pm, which is well outside the -3dB bandwidth of the amplifier.

3.5. VG Product Optimization

The results of sections 3.2 –3.4 demonstrate that the visibility, and thus coherence degree, of a VCSOA output can be accurately predicted when the gain saturation and light vs. current characteristics of the device are known. For our experiments, these were experimentally measured, but in principle could be generated using the Fabry-Perot gain equations and/or rate equations[13]. The visibility-gain product has been introduced as a figure of merit for VCSOAs used in coherent arrays. In this section, the functional trends of this product with input power and bias current are examined. The maximum of the VG product is found using the FP gain equations and parameters typical of the devices used. Plotted in Figure 9 is the VG product as a function of input power for several different bias currents. The highest curve represents a bias current 95% of the threshold current. The lowest curve is 80% of threshold, with 3% steps in between. The dashed curves are computed using a constant value for the ASE contribution, instead of the formalism of section 2.2. Two trends are evident in the product. First, the VG product increases with bias current due to the increasing gain. Secondly, the maximum value occurs at smaller power levels as bias current is increased. This is because an increase in bias current accelerates the rate at which the photon density builds up in the cavity, while only increasing the SE by a constant amount. Thus, the ratio of $I_{sp}/(GI_{in})$ in Eqn. 4 tends to zero more rapidly when the bias current is closer to threshold. The increase in gain also tends to lower the saturation power, and thus the ASE will be more quickly suppressed by the optical injection. However, the close agreement of the dashed lines demonstrates that the suppression of ASE is a minor effect.

4. CONCLUSIONS

The coherence degree (visibility) of a VCSOA has been characterized as a function of bias current, optical input power, and wavelength mismatch from the amplifier gain peak. Analytic expressions are available for the visibility and gain of the amplifier, and good agreement is obtained between theoretical calculations and experimental results. The VG product may be used as an optimization metric for choosing minimum input power levels and biasing condition. Several

general design rules for coherent arrays based on VCSOAs can be extracted from the results. First, the amplifier should be biased as close as practicable to the lasing threshold, since the increase in background emission is overcome by the increase in gain. Biasing close to the threshold will also allow for higher fan-out of a source, since acceptable correlation will be obtained at a smaller input power. Second, the linewidth of the source laser should be chosen to be much smaller than the gain bandwidth of the VCSOA, in order to minimize spectral distortion. Within the 3dB bandwidth of the amplifier, distortion has little effect on the visibility of the interference. A third conclusion is that the intensity of the input source should be well stabilized if small input power levels are used, since the visibility is a sensitive function of input flux below the saturation power level. The reduction of ASE from the amplifier with optical injection turns out to be a minor contribution. Though this effect must be included to achieve absolute agreement with measured results, it does not affect the trends and optimal operation conditions significantly.

REFERENCES

1. Pengyue Wen, Michael Sánchez, Osman Kibar, Sadik C. Esener "Low-voltage, high contrast-ratio, low-noise VCSEL modulator", OSA: *IPA/OAA*, Quebec, 2000.
2. Sánchez, M., et. al., "Phase Locked Vertical Cavity Surface Emitting Laser", *LEOS 2000*, Rio Grande, PR, 2000.
3. Lo, Y.T., "Array Theory," *Antenna Handbook*, Chp.11, New York: Van Nostrand Reinhold, 1993
4. Zakharov, S. M., "The Thermal Cross-Interference Effects in the Arrays of Vertical Cavity Surface Emitting Lasers", *Semiconductors*, **vol. 35**, pp.485-9, 2001.
5. Nakwaski, W., Osinski, M., "Thermal Resistance of Top-Surface Emitting Vertical Cavity Semiconductor Lasers and Monolithic Two-Dimensional Arrays", *Electronics Letters*, **vol. 28**, pp. 572-4, 1992
6. Hecht, E. *Optics*, 2nd Edition, pp. 516-529, Addison-Wesley Pub. Co., Inc., 1990
7. Guliani, G., et. al., "Noise Analysis of Gain-clamped and Conventional Semiconductor Optical Amplifiers", *Physics and Simulation of Optoelectronic Devices VIII*, p. 572-80, SPIE, San Jose, 2000
8. Voigt, D., et.al., "Characterization of a High-Power Tapered Semiconductor Amplifier System:, *Applied Physics B*, **vol. B72**, p. 279-84, 2001.
9. de Boer, A.P., et. al., "Amplified Spontaneous Emission Spectroscopy on Seminconductor Optical Amplifiers Subject to Active Light Injection", *Applied Physics Letters*, **vol. 72** , p. 2936-8, 1998.
10. Obermann, K., et. al., "Noise Analysis of Frequency Converters Utilizing Semiconductor-Laser Amplifiers", *IEEE Journal of Quantum Electronics*, **vol. 33**, pp.81-88, 1997
11. Tombling, C, et. al., "Performance Predictions for Vertical-Cavity Semiconductor Laser Amplifiers", *IEEE Journal of Quantum Electronics*, **vol. 30**, pp. 2491-99, 1994.
12. Mukai, T., Yamamoto, Y.Kimura, T., "Optical Amplification by Semiconductor Lasers", *Semiconductors and Semimetals*, Wilardson, R.K. and Beer, pp. 265-319, A.C., Academic, 1985.
13. Agrawal, G.P., Dutta, N.K., "Rate Equations and Operating Characteristics", *Semiconductor Lasers*, pp. 231-250, Kluwer Academic, 1993.